We are IntechOpen, the world's leading publisher of Open Access books Built by scientists, for scientists

4,800
Open access books available

122,000
International authors and editors

135M
Downloads

Our authors are among the

154
Countries delivered to

TOP 1%
most cited scientists

12.2%
Contributors from top 500 universities

CLARIVATE ANALYTICS BOOK CITATION INDEX INDEXED

WEB OF SCIENCE™

Selection of our books indexed in the Book Citation Index in Web of Science™ Core Collection (BKCI)

Interested in publishing with us?
Contact book.department@intechopen.com

Numbers displayed above are based on latest data collected.
For more information visit www.intechopen.com

10

A Haptically Enhanced Operational Concept for a Hydraulic Excavator

Henning Hayn and Dieter Schwarzmann
Robert Bosch GmbH
Germany

1. Introduction

In mobile hydraulic machines, like excavators, backhoe loaders, wheel loaders, and forklift trucks, haptic human-machine interfaces are not in use. Today, the machines are operated with mechanical-hydraulic joysticks. Each joystick axis controls a single hydraulic actuator. This leads to not very easy to use operational concepts. Since electrohydraulic systems with electronic joysticks are available for serial applications, alternative operational concepts become feasible.
A known alternative is to control the machine using an operating device whose segments resemble the manipulator geometry, as shown in Fig. 1 (Uchino et al., 1977). This operational concept is often called *coordinated control*. Typically, a master-slave system is employed where the operating device (master) outputs the reference position to the position control loop of the machine (slave). This concept promises an intuitive operation of the machine.

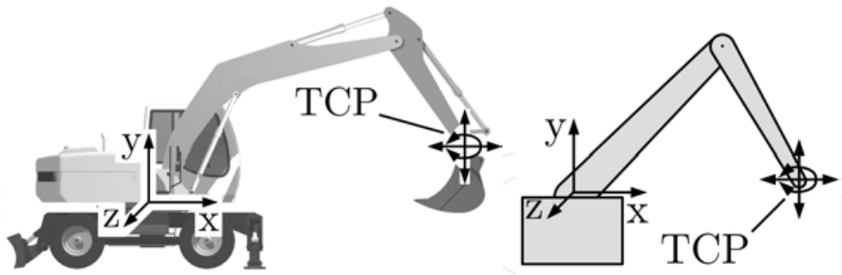

(a) Excavator (b) Operating device

Fig. 1. Operating device resembles the manipulator geometry

This concept can be enhanced by haptic assistance systems in order to improve the operator's performance. These haptically enhanced coordinated control operational concepts aim at

- increasing the machine efficiency (handling capacity) by providing driver assistance systems,
- reducing the time needed by the driver to learn the operation of the machine, and
- reducing operating errors especially for unexperienced drivers.

In this work, a SensAble Phantom Omni haptic device is used to generate the position reference signal for the tool center point (TCP) of the hydraulic manipulator of an 18 ton excavator. The two arm segments of the operating device resemble the boom and stick of the excavator, as shown in Fig. 2.

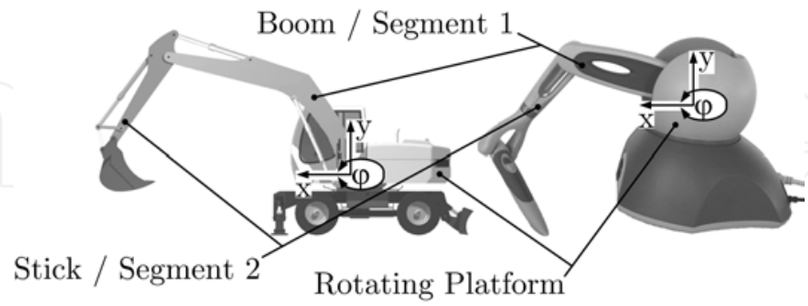

Fig. 2. Analogy of the geometry of a Phantom Omni device and an excavator manipulator

This chapter is organized as follows: Section 2 gives an overview of haptic feedback in mobile hydraulic machines. In Section 3 an alternative operational concept for excavators is proposed. Section 4 discusses the interconnection of the position controllers of the haptic device and the hydraulic excavator leading to a control methodology for bilateral master-slave systems. Section 5 introduces the applied controller design method, namely *internal model control* (IMC), for integrating plants with input constraints. After describing the controller design for the electric actuators of the haptic device and for the hydraulic actuators of the excavator, experimental results are given in Section 6. Section 7 shows the results of initial usability experiments with test drivers and Section 8 offers some conclusions.

2. Haptic Feedback in Mobile Hydraulic Machines

The automation level of available mobile machines is low, with the exception of some special applications like forest machines or robotic cargo loading systems. Due to the increasing use of automation technology, research and development activities focus on new human-machine interfaces and operational concepts. They aim at improving efficiency, safety and comfort. A prerequisite for innovative human-machine interfaces is the availability of electrohydraulics and the corresponding controllers. Then, new functions like driver assistance and safety systems can be integrated in the controller software as well as alternative operating devices. In the future, the level of automation in mobile machines will increase up to complete automation (Haas & Kim, 2002).
The integration of the sense of touch in the human-machine interface promises an easier, faster and more intuitive operation than the typically encountered visual information. Haptic interfaces have advantages, compared to human-machine interfaces that do not integrate the sense of touch, especially if the operator has to work delicately and accurately, or if various materials – for example with different elasticity – are handled.
Haptically enhanced assistance systems can support the driver of a mobile machine in performing his working task by providing tactile sensations via the operating device. Haptic driver assistance systems for hydraulic excavators could for example

- warn the driver of damaging obstacles,
- feed back digging or gripping forces,

- imitate open-center hydraulic systems,
- enable the driver to sense the inertia of the machine's manipulator,
- simplify leveling and slope cutting,
- limit the excavator's workspace,
- guide the bucket on a specific trajectory, or
- assist the collaborative manipulation of a heavy building element by multiple operators.

A significant advantage of haptic systems compared to semi- or fully automated assistance systems is, that the operator always has complete control over his machine. The driver is able to manually overrule the assistance systems, assuming that the human operator is always stronger than the actuators of the haptic device.
The application of haptic technologies in human-machine interfaces of mobile machines is not prior art in series-production vehicles. It can be found in some scientific contributions and sporadic industrial projects, only. One finds that either the machines are controlled with conventional force-feedback joysticks (Cemenska et al., 1989; Parker et al., 1993; Yamada & Muto, 2003; Augustine, 2005) or special haptic operating devices whose segments resemble the manipulator geometry (Ostoja-Starzewski & Skibniewski, 1989; Yoshinada & Takeda, 1990; Kraft, 1991; Kontz, 2007). The same principle is known from industrial robots and similar manipulators. An overview of haptic interface technology for mobile machines, like hydraulic excavators, can be found in Hayn & Schwarzmann (2008).

3. Development of an Intuitive Operational Concept for Hydraulic Excavators

Alternatives to conventional operational concepts are known but did not become widely accepted. The most important reasons are:

- Electrohydraulics was not available for series-production at reasonable prices,
- mechanical-hydraulic components are known for being robust and reliable, and
- the mobile machinery industry has a rather conservative attitude towards alternative operational concepts.

In order to design an intuitive operational concept for the hydraulic manipulator of excavators the coordinated control approach was developed further. It was assumed that operating elements that resemble the manipulator geometry are intuitive and easy to use. These operating elements have the same degree of freedom, the same types of joints and the same moving direction as the machine that has to be controlled. This property is called compatibility of the moving directions (Sachs et al., 1994). This means in detail for the manipulator of an excavator:

- The rotation of the cabin has to be controlled using a rotary operating element,
- the translation of the tool center point has to be controlled using an element which is free-moving within a vertical plane, and
- tilting the bucket has to be controlled using a rotary element.

The realization of this idea was expected to result in an unambiguous, predictable, and consistent, thus intuitive operational concept. When developing new operational concepts for hydraulic excavators it is additionally important to consider the concept being ergonomic and suitable for earthmoving machinery.

After evaluation of different configurations of operating elements on a virtual reality excavator simulator, the concept, shown on Fig. 3(a) as a virtual model, is proposed.
To improve the ergonomics the operating elements are scaled down to allow the manipulation via small motions of the right hand instead of the full arm. The operating elements are integrated into the arm rest to support effortless working. The sizes of the elements were adapted by polystyrene models. Unlike the original coordinated control concept here the operation of the manipulator is shared between both hands. The driver's left hand operates the rotation of the cabin. The right hand operates the position of the TCP in the x-y-plane on Fig. 2 and the bucket. It is possible to invert both elements to facilitate the use by left-handed persons. Fig. 3(b) shows the operating elements from the driver's point of view.

(a) Front view (b) Driver's view

Fig. 3. Intuitive operational concept for hydraulic excavators

The element for the operation of the TCP und the bucket is shown in detail on Fig. 4(a). The two main segments resemble the manipulator geometry. The bucket is controlled by swiveling the light gray, spring centered element. The slew drive for the rotating platform with the cabin is operated with the left hand using the turning knob shown in Fig. 4(b). The turning knob is divided into an inner dark gray disc and an outer light gray wheel. The inner disc can be used to set a desired swing angle. The outer wheel is used to control the yaw rate. The outer wheel allows positioning the rotating platform slowly and sensitively.
The operating elements are intended to be actuated in order to integrate haptically enhanced driver assistance systems according to Section 2.
The concept was tested on a virtual reality excavator simulator and on a real 18 ton wheel excavator. The proposed operational concept, which exists only as a virtual model, was evaluated using commercially available devices, namely a SensAble Phantom Omni device and a 3Dconnexion SpaceBall 5000, that are similar to the operating elements proposed before. The driver's right hand operates the SensAble Phantom Omni device. Unneeded degrees of freedom of the device, like the rotating platform, were locked into position. Instead of the turning knob the 3Dconnexion SpaceBall 5000 was used to set the reference yaw rate. Fig. 5 shows the operating devices mounted in the cabin of the test excavator.

(a) Element to operate the manipulator (b) Turning knob to rotate the cabin

Fig. 4. Enlarged view of the operating elements

4. Haptically Enhanced Master-Slave Control Methodology

4.1 Position Control Concept for Haptic Device and Excavator

The proposed operational concept is a typical bilateral master-slave system. The TCP of the hydraulic manipulator arm (slave) follows the reference signal of the operating element (master) on the right-hand side. However, in the case with an excavator as the slave, two issues appear: First, the human operator needs to sense how far the excavator lags behind the operating device. Without this information, it is difficult to accurately position the machine since the excavator moves significantly slower than the operator can move the operating device. Thus, without some sensory information, the operator cannot know how much lag to expect. Second, and more importantly, if the human operator releases the operating device (in steady-state), the excavator should not start to move. Otherwise, considering the case when the device is not actuated, the handle will fall if the user lets go and, consequently, the boom moves rapidly downwards as it follows the operating device. This behavior has to be avoided at all times. This leads to the assumption that the operating element necessarily has to be actuated. This was important for the technical realization of the proposed operational concept:

- The actuators are used to position-control the operating device in order to permanently synchronize its position with the position of the TCP of the excavator.
- The actuated device gives the possibility to feed back if the driver moves the operating element faster than the excavator can follow. This improves the handling quality of the machine.
- The actuators can be used to implement haptic driver assistance systems.

Fig. 6 shows the block diagram of a haptic human-machine interface for an electrohydraulic excavator including the human operator. Obviously, algorithms for the two controllers Q_{hd} and Q_{ex} have to be designed. The two controlled plants Σ are the haptic device (index hd) and the excavator (index ex). w denotes the reference variable, u the actuating variable and y the control variable, that is the output signal of each system. The physical representation (mechanical, electric, hydraulic) of each signal is given.

A control methodology for the proposed operational concept had to be found. Typical control concepts for bilateral teleoperator systems are based on the two-port network theory (Hannaford, 1989; Zhu & Salcudean, 1995; Salcudean et al., 1997; Tafazoli et al., 2002; Huang, 2004).

Fig. 5. Test excavator equipped with operating devices

This approach is not applicable to the presented problem because the operating device and the test excavator were not equipped with force sensors. Furthermore, transparency of the bilateral system was not required. Consequentially, an alternative control concept was adopted to solve the above-mentioned problems. The proposed solution is that two position controlled plants (excavator and haptic device) provide the reference position to each other, i.e., each system mirrors the position of the other system. Therefore, the operating device has to be actuated and position-controlled to mirror the current position of the excavator's arm. With this approach, if the user releases the handle in steady-state, it remains at its current position. Additionally, the haptic device will try to counteract the operator if it is moved away from its reference position. The operator can interpret the resulting force of the haptic device as an indication of the lag between the excavator and the operating device due to the inertia of the hydraulic manipulator.
The control methodology for the full master-slave system consisting of the haptic device and the excavator is shown in Fig. 7. Each plant output y_{hd} and y_{ex} is the reference signal for the other system, i.e., each system mirrors the actual position of the other system. This interconnected control loop works because the bandwidths of both systems differ significantly. The operator input w_{op} is modeled as an input disturbance d_{op} of the haptic device.
Position controllers for both systems – haptic device and excavator – are desired. Since the design method internal model control was utilized, as described later in Section 5 and 6, each controller Q consists of an internal model controller C and a prefilter F_{pre}. K_{hd} and K_{ex} are constant transformations

$$w_{\mathrm{ex}} = k_1 \cdot y_{\mathrm{hd}} + k_2 \tag{1}$$

$$w_{\mathrm{hd}} = \frac{1}{k_1} \cdot y_{\mathrm{ex}} - \frac{k_2}{k_1} \quad , \tag{2}$$

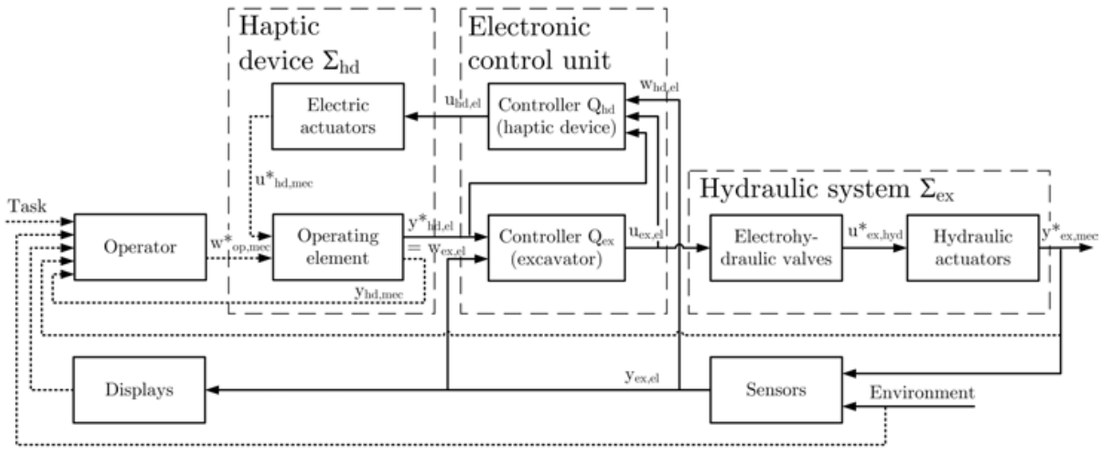

Fig. 6. Haptic human-machine interface of an excavator

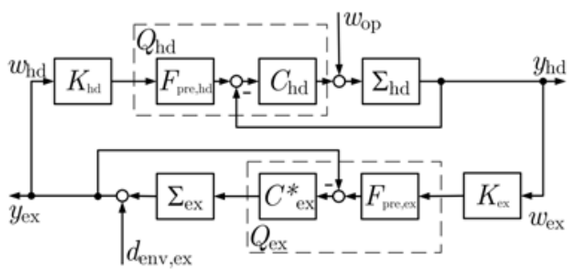

Fig. 7. Master-slave control loop

that convert the dimensions of the workspaces of one device to the other's. Internal stability of the system can be shown examining the poles of the relevant transfer functions.
The reference position is given in cylindrical coordinates: $w_{\mathrm{hd,x}}$, $w_{\mathrm{hd,y}}$, $w_{\mathrm{ex,x}}$, $w_{\mathrm{ex,y}}$ for the position of the TCP in a vertical plane (driven by boom and stick) and φ_{set} for the angle of the rotating platform (slew drive). The rotating platforms of both systems are single-input, single-output (SISO) plants. In order to control the position of the TCP, a reference signal generator is used. The reference signal generator converts the desired position into reference variables for the electric joint actuators φ_{ref} and the hydraulic cylinders $l_{\mathrm{ref,z1}}$, $l_{\mathrm{ref,z3}}$ using the inverse kinematics. In spite of the inaccuracy due to the static computation of the reference variables using the inverse kinematics, this approach provides the advantage that the joint actuators and cylinders can be treated as SISO systems and shows satisfactory experimental results.
Plants with static nonlinearities CC^{-1}, which are the hydraulic actuators including the valves, were treated by approximating them as Hammerstein models. The complete excavator control system is shown in Fig. 8.

4.2 Implementation of Haptically Enhanced Assistance Systems

The proposed control methodology implicates haptic feedback of the inertia of the hydraulic manipulator. Additional driver assistance systems like limiting the excavator's workspace or guiding the bucket on a specific trajectory are desired. These assistance systems can be implemented as virtual fixtures simulating stiff walls (Rosenberg, 1993; Burdea, 1996). Fig. 9 shows virtual walls within the workspace of the SensAble Phantom Omni. The an-

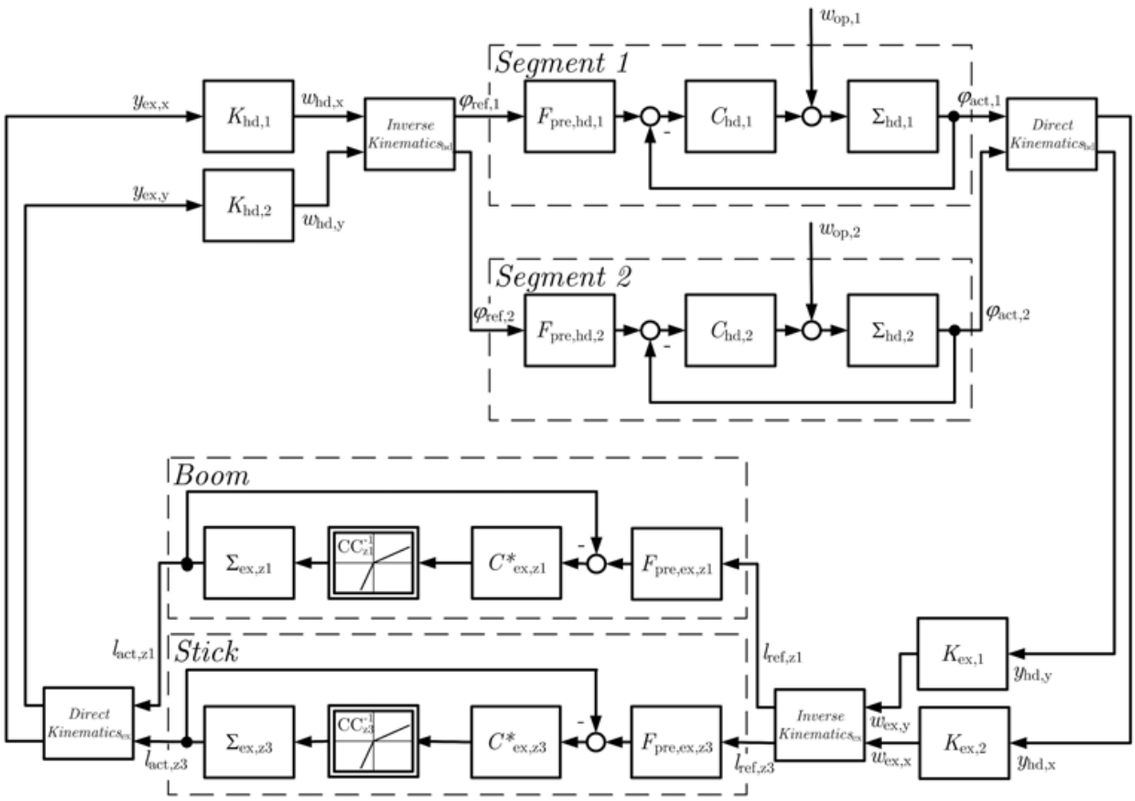

Fig. 8. Control loop implemented on the test excavator using a SISO architecture

gular wall in Fig. 9(a) supports the operator in slope cutting, the vertical wall haptically limits the workspace to protect the cabin of the excavator. Fig. 9(b) shows two walls building a slide rail that give the operator the feeling to be guided on a defined trajectory.
Usually, virtual walls are simulated as spring or spring-damper systems and implemented by adding a virtual force $\mathbf{f}_{\text{virtual}}$ via the controller of the haptic device. In this case, the actuators auf the haptic device are position- not force-controlled. Thus exerting such an external force onto the haptic device will interfere with the position controller which will lead to undesired results as the controller will try to counteract this seemingly undesired disturbance. In order to circumvent this problem, the method to constrain the actuating variable, introduced in Section 5.4, was applied to modulate the input constraints $u_{\text{hd,min}}$ and $u_{\text{hd,max}}$ dynamically to achieve a spring-like behavior. As a result, the position controller is made aware of the desired interference and will exert it on the haptic device itself. In a sense, the dynamic input constraints are used to tell the position controller how to incorporate the desired behavior into the running position control loop. The algorithm to calculate the constraints works as follows:

1. Computation of the spring force $\mathbf{f}_{\text{virtual}}$ which depends on the distance d between the TCP and the virtual wall:

$$\mathbf{f}_{\text{virtual}} = \begin{pmatrix} f_{\text{virtual,x}} \\ f_{\text{virtual,y}} \end{pmatrix} = k_{\text{wall}}\mathbf{n} = k_{\text{wall}} \begin{pmatrix} d_{\text{x}} \\ d_{\text{y}} \end{pmatrix} \quad . \tag{3}$$

   $\mathbf{n}$ is a normal vector with the length d.

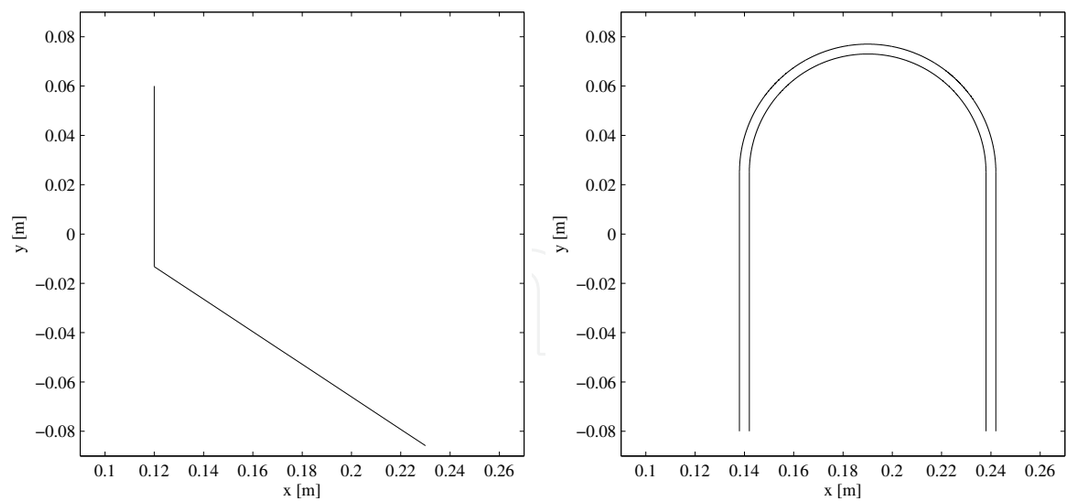

(a) Slope assistance and workspace limitation (b) Trajectory guidance

Fig. 9. Virtual walls within the workspace of the haptic device

2. If the TCP penetrates the virtual wall ($d \leq 0$) two moments M_{virtual} for both segments of the operating element are calculated:

$$M_{\text{virtual},1} = u_{\text{hd,feedback},1} = \frac{k_{\text{wall}}}{l_1} \cdot \frac{d_{\text{x}} \sin\varphi_2 - d_{\text{y}} \sin\varphi_2}{\sin\varphi_1 \sin\varphi_2 + \cos\varphi_1 \cos\varphi_2} \tag{4}$$

$$M_{\text{virtual},2} = u_{\text{hd,feedback},2} = \frac{k_{\text{wall}}}{l_2} \cdot \frac{-d_{\text{x}} \cos\varphi_1 - d_{\text{y}} \sin\varphi_1}{\sin\varphi_1 \sin\varphi_2 + \cos\varphi_1 \cos\varphi_2} \quad . \tag{5}$$

These moments generate the desired force at the TCP. The equation results from the kinematics of the haptic device. l and φ denote the lengths and angles as shown in Fig. 10. These calculated moments and the actuating variable u_{hd} of the electric actuators of the device are proportional ($M_{\text{virtual}} \sim u_{\text{hd}}$). Hence the actuating variable to generate the desired force $\mathbf{f}_{\text{virtual}}$ via these moments is called $u_{\text{hd,feedback}}$.

3. The constraints $u_{\text{hd,min}}$ and $u_{\text{hd,max}}$ of the actuating variables of both segments are

$$u_{\text{hd,min}} = u_{\text{hd,limit,min}} + u_{\text{hd,gravity}} + u_{\text{hd,feedback}} \quad , \tag{6}$$

$$u_{\text{hd,max}} = u_{\text{hd,limit,max}} + u_{\text{hd,gravity}} + u_{\text{hd,feedback}} \quad . \tag{7}$$

$u_{\text{hd,limit}}$ is the physical input constraint of each plant according to Section 5.4. $u_{\text{hd,gravity}}$ is a constant that compensates the influence of gravity on the haptic device even if the control deviation is null. The constraints $u_{\text{hd,min}}$ and $u_{\text{hd,max}}$ are applied according to Equations (30) and (31).

The adopted constraints force the haptic device to behave like a stiff spring if the TCP is within the predefined fixtures. After adjusting k_{wall} in experiments this approach showed good results. The simulated stiff wall can be sensed easily.

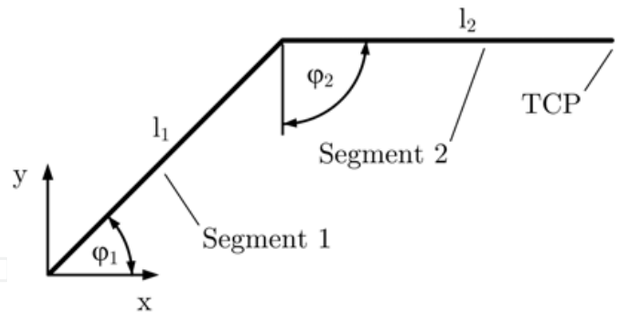

Fig. 10. Kinematics of a SensAble Phantom Omni

5. Internal Model Control of Linear SISO Systems

The proposed control methodology in Fig. 8 demands several controllers, one for each plant in both systems. Since both types of plants (electric joint actuators of the SensAble Phantom Omni device as well as the hydraulic cylinders and the slew drive of the excavator) show an integrating behavior, the same control method, namely internal model control for integrating linear SISO systems, is chosen for all plants. A review of the design is given in the following, starting with non-integrating plants, i.e., plants Σ having i poles p_i with $\mathrm{Re}\{p_i\} < 0$ for all i.

5.1 IMC for Non-Integrating Stable Systems

The main idea of IMC is to include a model $\tilde{\Sigma}$ of the plant Σ into the controller K, as shown in Fig. 11. If $\tilde{\Sigma}$ models the plant Σ exactly and in the absence of disturbances ($d = 0$), the feedback signal equals zero ($y(t) - \tilde{y}(t) = 0$), and the IMC controller Q is a feed-forward controller.

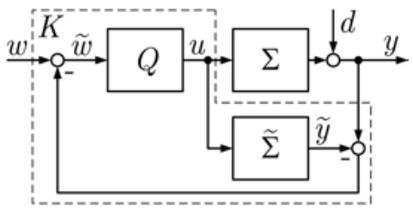

Fig. 11. IMC structure

The IMC controller Q is a series connection of a filter F and the inverse model $\tilde{\Sigma}^{-1}$:

$$Q = F\tilde{\Sigma}^{-1} \quad . \tag{8}$$

For non-integrating plants, in Frank (1974) and Morari & Zafiriou (1989), the following structure for the filter F is proposed:

$$F(s) = \frac{1}{(\frac{1}{\lambda}s + 1)^r} \quad \text{with} \quad \lambda > 0 \quad , \tag{9}$$

where λ is a design parameter and r is the relative degree of $\tilde{\Sigma}$.
The IMC structure can always be converted into the standard control loop shown in Fig. 12 (Schwarzmann, 2007):

$$C = \frac{1}{1-F}Q = \frac{F}{1-F}\tilde{\Sigma}^{-1} = F_{\text{tot}}\tilde{\Sigma}^{-1} \quad . \tag{10}$$

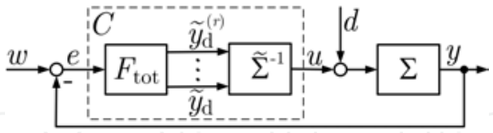

Fig. 12. IMC structure implemented in a standard control loop

The separation of the controller C into a filter F_{tot} and the inverse of a model $\tilde{\Sigma}^{-1}$ is required for the proposed limitation of the controller output u in Section 5.4.

5.2 IMC for Integrating Systems

The previously proposed filter F in Equation (9) and the resulting filter F_{tot} are not sufficient for integrating systems because step input disturbances d lead to a steady-state offset (Morari & Zafiriou, 1989). The filter F_{tot} has to have at least the same relative degree as $\tilde{\Sigma}$ and $i+1$ pure integrators (i.e. poles at zero) in order to design a proper controller C, where i is the number of pure integrators of the plant model $\tilde{\Sigma}$. According to the design procedure presented in Morari & Zafiriou (1989), a system of linear equations has to be solved to determine the filter F for this type of plants. To avoid this difficulty, a modified design rule for F is introduced to design an internal model controller for integrating linear minimum phase systems in a standard control loop. This modified design rule leads to the same result as the proposed solution by Morari & Zafiriou (1989) but in a single step as opposed to solving a system of equations.
To generate the desired filter F_{tot} from the positive feedback loop of F (cf. Equation (10)), F is chosen in such a manner that terms $\delta_i s^i$ up to the i-th order of the denominator polynomial of F are canceled by subtracting the numerator. The corresponding filter F is

$$\begin{aligned} F(s) &= \frac{\frac{\gamma_i}{\lambda^i}s^i + \frac{\gamma_{i-1}}{\lambda^{i-1}}s^{i-1} + \ldots + \frac{\gamma_2}{\lambda^2}s^2 + \frac{\gamma_1}{\lambda}s + 1}{\frac{\gamma_{r+i}}{\lambda^{r+i}}s^{r+i} + \ldots + \frac{\gamma_i}{\lambda^i}s^i + \ldots + \frac{\gamma_1}{\lambda}s + 1} \\ &= \frac{\delta_i s^i + \delta_{i-1}s^{i-1} + \ldots + \delta_2 s^2 + \delta_1 s + 1}{(\frac{1}{\lambda}s+1)^{r+i}} \\ &\text{with} \quad \delta_n = \frac{\gamma_n}{\lambda^n} \quad , \quad 0 \le n \le i \quad . \end{aligned} \tag{11}$$

The numerator of F consists of all terms up to the i-th order of the polynomial of the extended denominator of F ($(\frac{1}{\lambda}s+1)^{r+i}$), which are the last $i+1$ summands of the denominator. λ is a design parameter, r is the relative degree of $\tilde{\Sigma}$, γ and δ are constant coefficients. F_{tot} is then

$$
\begin{aligned}
F_{\mathrm{tot}}(s) &= \frac{F}{1-F} = \frac{\mathrm{numerator}(F)}{\mathrm{denominator}(F) - \mathrm{numerator}(F)} \\
&= \frac{\delta_i s^i + \delta_{i-1} s^{i-1} + \ldots + \delta_2 s^2 + \delta_1 s + 1}{(\frac{1}{\lambda} s + 1)^{r+i} - \delta_i s^i - \ldots - \delta_2 s^2 - \delta_1 s - 1} \\
&= \frac{\frac{\gamma_i}{\lambda^i} s^i + \frac{\gamma_{i-1}}{\lambda^{i-1}} s^{i-1} + \ldots + \frac{\gamma_2}{\lambda^2} s^2 + \frac{\gamma_1}{\lambda} s + 1}{\frac{\gamma_{r+i}}{\lambda^{r+i}} s^{r+i} + \ldots + \frac{\gamma_{i+1}}{\lambda^{i+1}} s^{i+1}} \\
&= \frac{\frac{\gamma_i}{\lambda^i} s^i + \frac{\gamma_{i-1}}{\lambda^{i-1}} s^{i-1} + \ldots + \frac{\gamma_2}{\lambda^2} s^2 + \frac{\gamma_1}{\lambda} s + 1}{s^{i+1}(\frac{\gamma_{r+i}}{\lambda^{r+i}} s^r + \frac{\gamma_{r+i-1}}{\lambda^{r+i-1}} s^{r-1} + \ldots + \frac{\gamma_{i+1}}{\lambda^{i+1}})} \quad .
\end{aligned} \tag{12}
$$

This results in the desired number of integrators in F_{tot}. The tuning parameter λ determines the resulting bandwidth of the closed loop. The specified design rule for F_{tot} allows to follow ramp reference signals and removes the steady-state offset in the case of step input disturbances.

5.3 Prefilter Design

A prefilter F_{pre} is introduced to reduce overshoot. This leads to a second degree of freedom to parameterize the behavior of the closed loop.
If $\tilde{\Sigma}$ is an ideal model of the plant Σ, the transfer behavior of the closed loop system is equal to the filter F (see Fig. 11). Hence the desired behavior F_{d} of the system can be forced by the prefilter

$$
F_{\mathrm{pre}} = F_{\mathrm{d}} F^{-1} \quad . \tag{13}
$$

The desired behavior F_{d} is usually a low-pass filter

$$
F_{\mathrm{d}} = \frac{1}{(\frac{1}{\lambda_{\mathrm{d}}} s + 1)^{r_{\mathrm{d}}}} \tag{14}
$$

with the design parameter λ_{d}. This holds if r_{d} is greater than or equal to the relative degree of F.

5.4 Input Constraints

In technical systems, the actuating variable u is limited: $u \in [u_{\min}, u_{\max}]$. When neglected, this input constraint of the plant can lead to undesirable windup effects. Especially the haptic device shows these effects because of the persistent integration of the position error variable due to the operator holding the handle of the device. If not treated by the control algorithm, the result is a strong integral windup effect if the user releases the handle of the haptic device. Due to the design specifications overshoot is not desired. Therefore, a windup compensation according to Schwarzmann (2007) was designed as follows:
If the IMC controller Q is implemented as a series connection of F and the inverse of the plant model $\tilde{\Sigma}^{-1}$ (cf. Fig. 12), a constraint of the highest derivative $\tilde{y}_d^{(r)}$ of the filter output limits the output u of the controller. Using this structure, the filter F forces a desired behavior $\tilde{y}_d$ of the plant that does not violate the input constraints $u_{\min}$ and $u_{\max}$ of the plant Σ.
According to Graichen & Zeitz (2006) the inverse of a model $\tilde{\Sigma}$ can be determined as follows: A controllable model $\tilde{\Sigma}$

$$\tilde{\Sigma}: \quad \dot{x} = \boldsymbol{f}(\boldsymbol{x}, u), \quad \boldsymbol{x}(0) = \boldsymbol{x}_0, \quad \tilde{y} = h(\boldsymbol{x}) \tag{15}$$

with a relative degree r, defined as

$$r = \arg\min_k \{ \frac{\partial}{\partial u} L_f^k h(\boldsymbol{x}, u) \neq 0 \} \quad , \tag{16}$$

where $L_f h$ means the Lie-derivative of h with respect to f, can be transformed to the nonlinear normal form

$$\tilde{y}^{(r)} = \alpha(\tilde{y}, \dot{\tilde{y}}, \ldots \tilde{y}^{(r-1)}, \boldsymbol{\eta}, u) \tag{17a}$$

$$\dot{\eta} = \boldsymbol{\beta}(\boldsymbol{\eta}, \tilde{y}, \dot{\tilde{y}}, \ldots \tilde{y}^{(r-1)}, u) \tag{17b}$$

with $\alpha(\cdot) = L_f^r h \circ \boldsymbol{\phi}^{-1}$ and $\beta(\cdot) = L_f \phi_{n,i} \circ \boldsymbol{\phi}^{-1}$ using the state transformation

$$[\tilde{y}, \dot{\tilde{y}}, \ldots \tilde{y}^{(r-1)}, \boldsymbol{\eta}]^T = \boldsymbol{\phi}(\boldsymbol{x}) \quad \text{with} \tag{18a}$$

$$\tilde{y}^{(i)} = L_f^i h(\boldsymbol{x}) = \phi_{i+1}, \quad i = 0, \ldots, r-1 \tag{18b}$$

$$\boldsymbol{\eta} = \boldsymbol{\phi}_\eta(\boldsymbol{x}) \in \mathbb{R}^{n-r} \quad . \tag{18c}$$

The inverse of the model $\tilde{\Sigma}$ is then

$$\tilde{\Sigma}^{-1}: \quad u = \alpha^{-1}(\tilde{y}_d, \dot{\tilde{y}}_d, \ldots \tilde{y}_d^{(r)}, \boldsymbol{\eta}) \tag{19a}$$

$$\dot{\eta} = \boldsymbol{\beta}(\boldsymbol{\eta}, \tilde{y}_d, \dot{\tilde{y}}_d, \ldots \tilde{y}_d^{(r-1)}, u) \quad , \tag{19b}$$

where the function α^{-1} is the solution of Equation (17a) for u.
For linear systems $\tilde{y} = \tilde{\Sigma} u$ without zeros, the controller output $u = \tilde{\Sigma}^{-1} \tilde{y}$ can be described as

$$u = u(\tilde{y}_\mathrm{d}, \dot{\tilde{y}}_\mathrm{d}, \ldots, \tilde{y}_\mathrm{d}^{(r-1)}, \tilde{y}_\mathrm{d}^{(r)}) = a_0 \tilde{y}_\mathrm{d} + a_1 \dot{\tilde{y}}_\mathrm{d} + \ldots + a_{(r-1)} \tilde{y}_\mathrm{d}^{(r-1)} + a_r \tilde{y}_\mathrm{d}^{(r)} \quad . \tag{20}$$

For the above-named systems with i integrators at the plant output, the controller output u is not a function of the desired behavior $\tilde{y}_\mathrm{d}$ and its first $i-1$ derivatives

$$u = u(\tilde{y}_\mathrm{d}^{(i)}, \tilde{y}_\mathrm{d}^{(i+1)}, \ldots, \tilde{y}_\mathrm{d}^{(r-1)}, \tilde{y}_\mathrm{d}^{(r)}) = a_i \tilde{y}_\mathrm{d}^{(i)} + a_{i+1} \tilde{y}_\mathrm{d}^{(i+1)} + \ldots + a_{(r-1)} \tilde{y}_\mathrm{d}^{(r-1)} + a_r \tilde{y}_\mathrm{d}^{(r)} \quad . \tag{21}$$

Note that this is an algebraic equation. To obtain the necessary derivatives $\tilde{y}_d^{(r)}$ for the inverse of the model, the filter F was implemented as a state-variable filter (SVF) as shown in Fig. 14. This structure allows to limit the highest derivative $\tilde{y}_d^{(r)}$ in order to constrain the actuating variable u.
The limits $\tilde{y}_{\mathrm{d,min}}^{(r)}$ and $\tilde{y}_{\mathrm{d,max}}^{(r)}$ can be calculated by solving Equation (19a) for $\tilde{y}^{(r)}$ and using Equation (21):

$$\tilde{y}_{\mathrm{d,min}}^{(r)} = \min_{u \in [u_{\min}, u_{\max}]} (\bar{\alpha}(\tilde{y}_\mathrm{d}, \dot{\tilde{y}}_\mathrm{d}, \ldots, \tilde{y}_\mathrm{d}^{(r-1)}, u)) \tag{22a}$$

$$\tilde{y}_{\mathrm{d,max}}^{(r)} = \max_{u \in [u_{\min}, u_{\max}]} (\bar{\alpha}(\tilde{y}_\mathrm{d} d, \dot{\tilde{y}}_\mathrm{d}, \ldots, \tilde{y}_\mathrm{d}^{(r-1)}, u)) \quad . \tag{22b}$$

This means that the actuating variable u is constrained exactly to $[u_{\min}, u_{\max}]$ if the highest derivative $\tilde{y}_{\mathrm{d}}^{(r)}$ is restricted to these limits.

6. Controller Design for the Operating Device and for the Excavator

6.1 Design Procedure

The controllers in Fig. 8 were designed utilizing the IMC method. The following procedure was used to design the IMC controllers for the haptic device (electric motors) and the excavator (electrohydraulic valves to control the boom, stick, and bucket cylinders):

1. Take measurements of the static and dynamic behavior of the plant Σ (gain and step response)
2. Parameter identification of the parametric model in Equation (23) for each actuator
3. IMC controller design using the parameterized models
4. Design of a prefilter to minimize overshoot

This approach allows a straightforward controller development. The prefilters in Fig. 8 are needed since a large peak overshoot is not acceptable due to safety reasons: The excavator boom is not allowed to exceed its reference position because it could damage objects close to the bucket. The additional prefilter converts the structure to a two-degrees-of-freedom controller.
To this end, the plant models were chosen as an integrator and a first-order filter:

$$\tilde{\Sigma} = \frac{k}{s(Ts+1)} \quad , \tag{23}$$

where parameter k is the gain and T is the time constant of the low-pass filter. The model parameters were determined by measurements. The controllers C and prefilters F_{pre} were designed according to Section 5.

6.2 Controller Design for the Haptic Device

The actuating variables for the SensAble Phantom Omni haptic device are the motor currents of each joint. The output variables are the joint angles. Fig. 13 shows the step response of the first segment and the actuating variable $u_{\mathrm{hd},1}$. The actuating variable does not return to zero as the effect of gravity requires the electric motors of the haptic device to be actuated permanently to hold their positions.
As mentioned before, the controller of the haptic device requires an anti-windup strategy according to Section 5.4. As a consequence, F_{tot} was implemented as the state-variable filter shown in Fig. 14. The used filter F_{tot}

$$F_{\mathrm{tot}} = \frac{\delta_1 s + 1}{\delta_3 s^3 + \delta_2 s^2} \tag{24}$$

leads to the differential equation

$$y_d^{(3)} + \frac{\delta_2}{\delta_3} y_d^{(2)} = \frac{\delta_1}{\delta_3} u^{(1)} + \frac{1}{\delta_3} u \quad . \tag{25}$$

The system can also be described in controllable standard form (Lunze, 2006) as

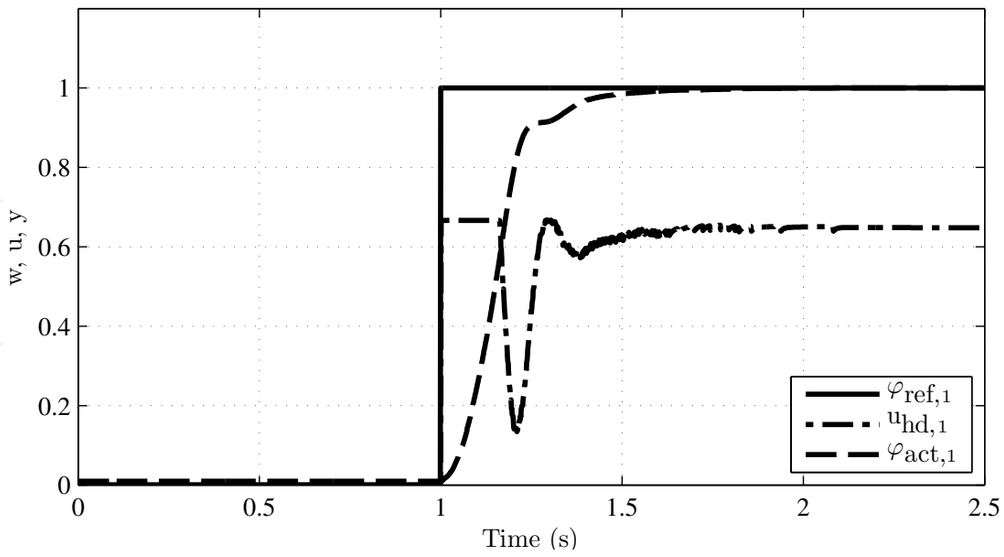

Fig. 13. Step response of the first segment of the haptic device

$$\dot{\boldsymbol{x}}_{\mathrm{tr}} = \begin{pmatrix} 0 & 1 & 0 \\ 0 & 0 & \frac{\delta_3 - \delta_1\delta_2}{\delta_3^2} \\ 0 & 0 & -\frac{\delta_2}{\delta_3} \end{pmatrix} \boldsymbol{x}_{\mathrm{tr}} + \begin{pmatrix} 0 \\ \frac{\delta_1}{\delta_3} \\ 1 \end{pmatrix} u \tag{26}$$

$$\tilde{y}_d = \begin{pmatrix} 1 & 0 & 0 \end{pmatrix} \boldsymbol{x}_{\mathrm{tr}} \tag{27}$$

by using the transformation $\boldsymbol{x}_{\mathrm{tr}} = \boldsymbol{T}_{\mathrm{R}}\boldsymbol{x}$ with

$$\boldsymbol{T}_{\mathrm{R}} = \begin{pmatrix} \frac{1}{\delta_3} & \frac{\delta_1}{\delta_3} & 0 \\ 0 & \frac{1}{\delta_3} & \frac{\delta_1}{\delta_3} \\ 0 & 0 & 1 \end{pmatrix} \quad . \tag{28}$$

The transformed system can be implemented as the block diagram shown in Fig. 14. Note the integrator chain at the output of F_{tot}.
The algebraic model of each actuated segment j of the operating element is

$$k_{\mathrm{j}} \cdot \ddot{y}_{\mathrm{hd,j}} + \dot{y}_{\mathrm{hd,j}} = T_{\mathrm{j}} \cdot u_{\mathrm{hd,j}} \quad . \tag{29}$$

Utilizing the algebraic model Σ_{hd} allows to compute the constraints for the highest derivative $\ddot{y}_{\mathrm{hd}}$ according to Section 5.4:

$$\ddot{y}_{\mathrm{hd,min}} = \frac{1}{k_{\mathrm{j}}}(-\dot{y}_{\mathrm{hd}} + T_{1,\mathrm{j}} \cdot u_{\mathrm{hd,min}}) \quad , \tag{30}$$

$$\ddot{y}_{\mathrm{hd,max}} = \frac{1}{k_{\mathrm{j}}}(-\dot{y}_{\mathrm{hd}} + T_{1,\mathrm{j}} \cdot u_{\mathrm{hd,max}}) \quad . \tag{31}$$

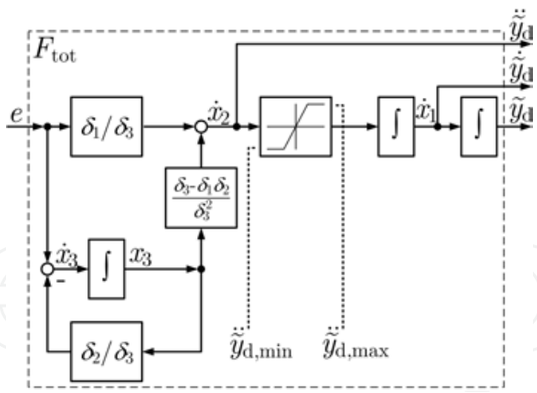

Fig. 14. State-variable filter for the haptic device controller including input constraints

6.3 Controller Design for the Hydraulic Boom

The actuating variables for the hydraulic cylinders of the excavator are the flow rates of the hydraulic oil that the valves distribute to each cylinder or to the slew drive. The output variables are the cylinder positions or the angle of the rotating platform, respectively. Fig. 15 shows the step response of the boom cylinder and the actuating variable $u_{\text{ex,z1}}$.

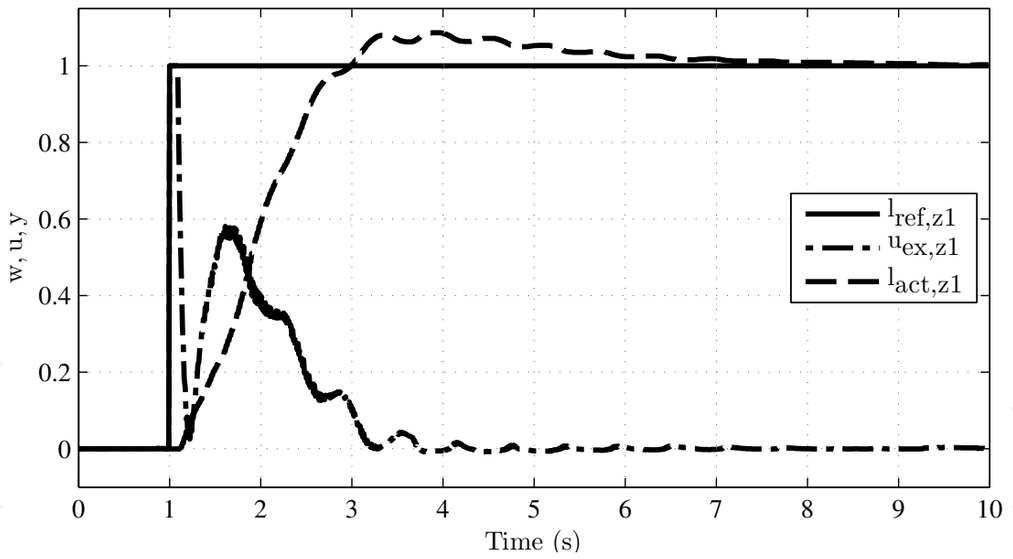

Fig. 15. Step response of the excavator's boom cylinder

Model errors result in an acceptable overshoot. The oscillations of the machine on its tyres can be seen in the measurements.

6.4 Experimental Results

The master-slave control approach introduced in Section 4 shows satisfying results in experiments on the test excavator. The controller for the SensAble Phantom Omni device was running under MATLAB/Simulink. The boom controller was implemented on dSPACE proto-

typing hardware. Position sensors for the hydraulic cylinders and an angular rate sensor for the rotating platform were utilized to measure the actual position of the machine.
The step response of the x-y-controlled hydraulic arm in the horizontal direction x is shown on Fig. 16 (a). The position error in the vertical direction y is less than $\pm$ 0.05 m (cf. Fig. 16 (b)).

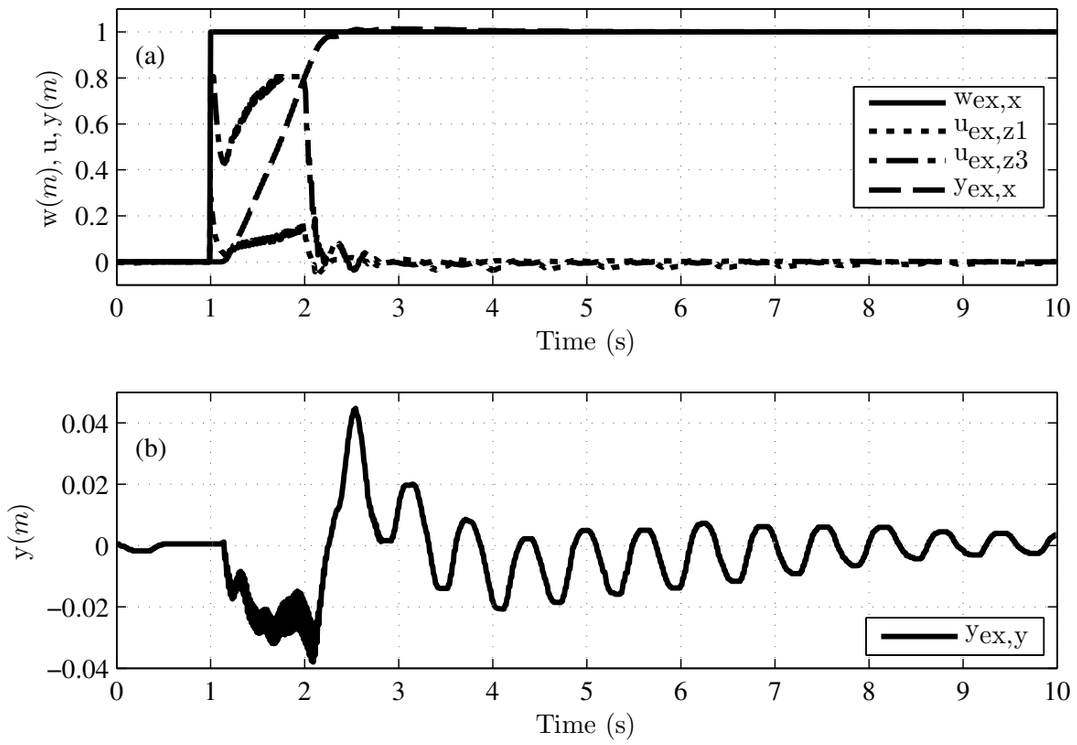

Fig. 16. Step response of the hydraulic arm

The behavior of the interconnected master-slave system is shown on Fig. 17. The position signals $w_{\text{ex,x}}$ and $w_{\text{ex,y}}$ of the haptic device are low-pass filtered. This was necessary to achieve a smooth reference signal for the excavator. The operator used the haptic device to prescribe the curve in Fig. 18.

7. Evaluation of the Haptically Enhanced Operational Concept

Goal of the proposed operational concept is to improve the handling quality and to simplify the operation — especially for untrained drivers. This target was evaluated by usability experiments with test operators. The configuration using a SensAble Phantom Omni and a 3Dconnexion SpaceBall 5000, as shown in Fig. 5, was used to proof this concept. Twelve male test operators without any relevant experience with hydraulic excavators performed a predefined working task. They were filmed to analyze the working cycle times and operating errors. Finally the test persons were surveyed using a questionnaire.

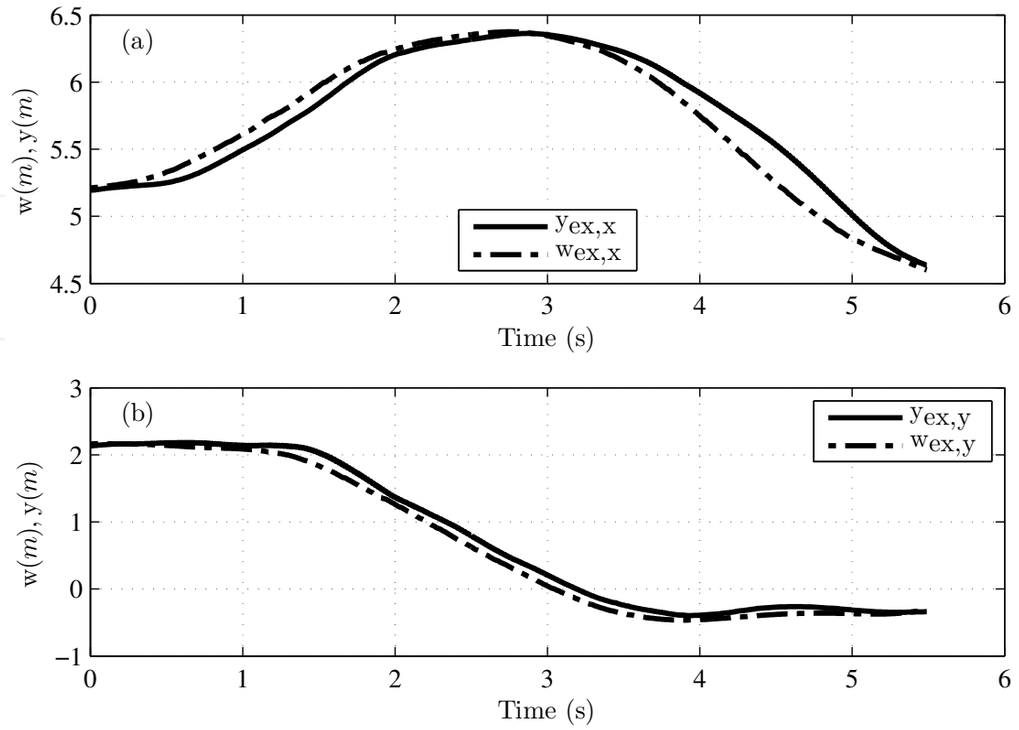

Fig. 17. Position on x- and y-axis of the excavator and the haptic device over time

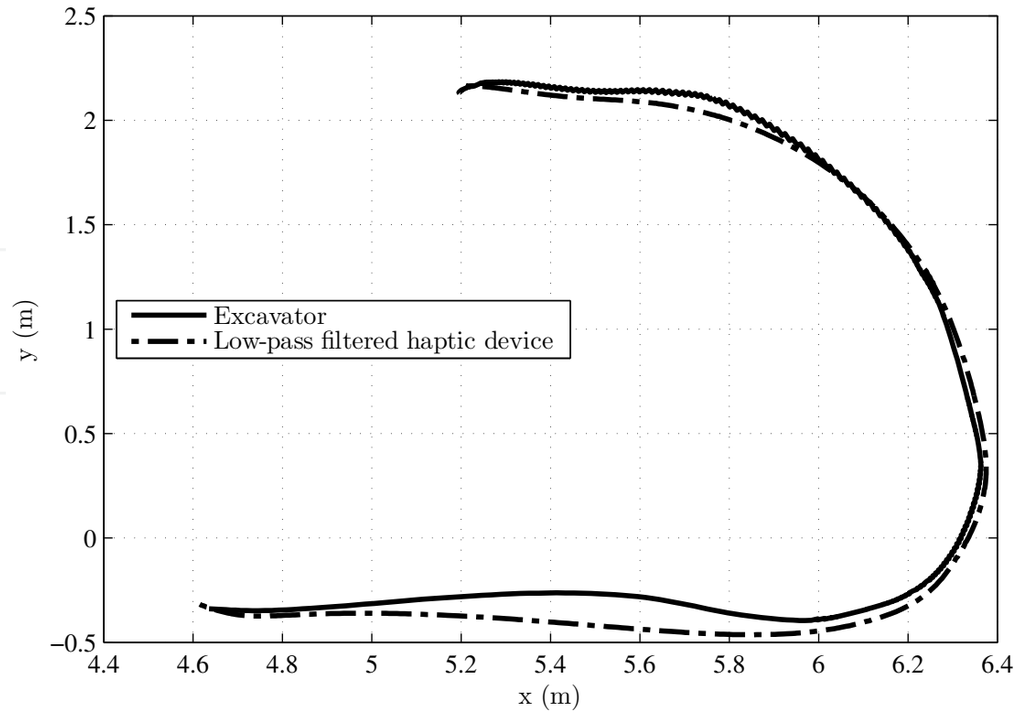

Fig. 18. TCP-position of the haptic device and the excavator

7.1 Intuitive Operational Concept

The test operators started with performing a typical working task using the standard joysticks. After this run, they performed the same tasks using the new concept. The time to complete a working cycle and the operating errors were compared. An operating error is a motion of the excavator's TCP into the wrong direction due to a wrong operator input. These errors were easily seen due to the predefined task. Reasons for errors are confusions of operating elements or joystick axes. The typical working cycle consisted of

- loading the bucket with soil,
- rotating the cabin about 90° and lifting the bucket over an obstacle,
- unloading the soil,
- moving back to the initial position and starting the next cycle.

Before starting, the test operators got a brief instruction to the hydraulic excavator and the operational concepts. Since some learning effects can be observed already after a short time only the first two cycles of each operator were analyzed. It was assumed that short cycle times and less operating errors are indicators for an intuitive operational concept. A paired t-test was calculated for the cycle times ($t(11) = -3.324; p = 0.007$) and for the operating errors ($t(11) = -6.588; p = 0.000$). The results in Fig. 19 show significant differences between both operational concepts. The cycle time and especially the number of errors are significantly lower. These results coincide with related studies by Wallersteiner et al. (1993) and Lawrence et al. (1990). The survey showed that the inexperienced operators subjectively benchmark the coordinated control concept better than the standard control concept regarding usability and training time.

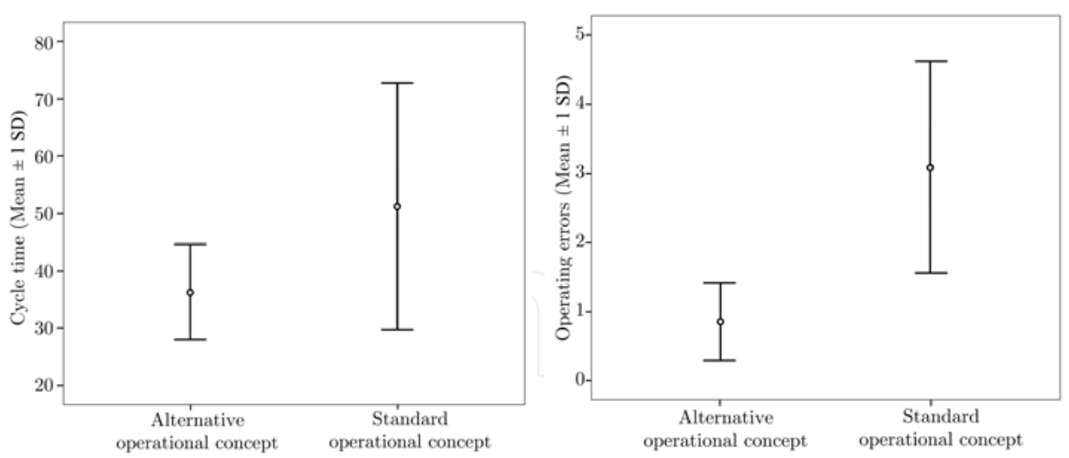

(a) Cycle time (b) Operating errors

Fig. 19. Evaluation of the proposed operational concept

7.2 Haptically Enhanced Driver Assistance Systems

Fig. 20 illustrates the implemented haptic driver assistance systems for slope leveling and trajectory guidance according to Fig. 9. Fig. 20(a) shows the position y_{ex} of the hydraulic manipulator's TCP. It was necessary to filter the signal y_{hd} in order to eliminate the high-frequency

jittering of the operator's hand before using it as reference signal w_{ex} for the excavator. Note that the operator can easily follow the predefined slope without penetrating the virtual fixtures. The repeat accuracy is less than 0.1 m. In the workspace right of the virtual wall the operating device can move freely. A measurement of the trajectory guidance system is shown in Fig. 20(b). The operator is guided on a predefined trajectory. A noticeable high force is needed to leave this path.

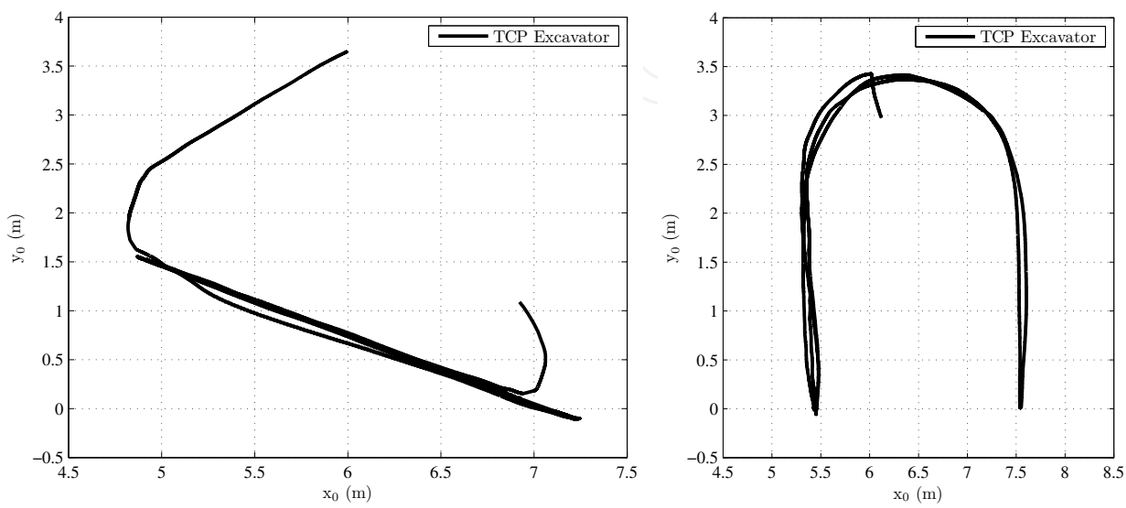

(a) Slope assistance (b) Trajectory guidance

Fig. 20. Measurements of the implemented haptic driver assistance systems

The test operators evaluated the haptically enhanced assistance systems as very expedient and helpful.

8. Conclusion

An intuitive operational concept for a hydraulic excavator was proposed. A conceptual design for an alternative operating device for excavators was developed. In order to implement this concept on a test excavator, an IMC-based control methodology was used and extended where necessary. An introduction to internal model control with input constraints for a haptic device and a feedback control methodology for a master-slave system were presented. An anti-windup approach for models with pure integrators is proposed. This approach is extended to implement haptic feedback. The application was tested in experiments using a SensAble Phantom Omni device and a hydraulic test excavator.

This work shows a straightforward control method to manipulate a machine using an active operating device that resembles the boom geometry. The approach can be applied to similar master-slave systems, e.g. for teleoperation.

The user is able to feel the inertia of the excavator's manipulator and thus gets feedback on the interaction of the bucket with the environment. Haptically enhanced assistance systems for tactile workspace limitations, leveling of soil and guidance on specific trajectory are integrated.

Future work has to be the development of working prototypes of the proposed operating elements, including actuators. These prototypes have to be robust and suitable for mobile

machines. Extensive usability tests should be performed with that system to ensure the concept.
Additionally, the haptic device and the test excavator could be equipped with force sensors to allow testing of further bilateral control concepts.

9. References

Augustine, A. W. (2005). Tactile feedback system for a remotely controlled work machine, *Patent US 6836982 B1*, Caterpillar Inc.

Burdea, G. C. (1996). *Force and Touch Feedback for Virtual Reality*, John Wiley & Sons, Inc., New York.

Cemenska, R. A., Schneider, M. P. & Buege, T. J. (1989). Force feedback lever, *Patent US 4800721*, Caterpillar Inc.

Frank, P. M. (1974). *Entwurf von Regelkreisen mit vorgeschriebenem Verhalten*, G. Braun Verlag, Karlsruhe.

Graichen, K. & Zeitz, M. (2006). Inversionsbasierter Vorsteuerungsentwurf mit Ein- und Ausgangsbeschränkungen, *Automatisierungstechnik* **54**(4): 187–199.

Haas, C. T. & Kim, Y.-S. (2002). Automation in infrastructure construction, *Construction Innovation* **2**: 191–210.

Hannaford, B. (1989). A design framework for teleoperators with kinesthetic feedback, *IEEE Transactions on Robotics and Automation* **5**(4): 426–434.

Hayn, H. & Schwarzmann, D. (2008). Haptic feedback for mobile machines, *6th International Fluid Power Conference*, Vol. 1, Institut für Fluidtechnik, Technische Universität Dresden, Dresdner Verein zur Förderung der Fluidtechnik e. V. Dresden, Dresden.

Huang, P. (2004). *Regelkonzepte zur Fahrzeugfhrung unter Einbeziehung der Bedienelementeigenschaften*, PhD thesis, TU Mnchen.

Kontz, M. E. (2007). *Haptic Control of Hydraulic Machinery Using Proportional Valves*, PhD thesis, G.W. Woodruff School of Mechanical Engineering, Georgia Institute of Technology.

Kraft, B. W. (1991). Force feedback control for backhoe, *Patent US 5019761*.

Lawrence, P., Sauder, B., Wallersteiner, U. & Wilson, J. (1990). Teleoperation of forest harvesting machines, *in* J. Coutteau (ed.), *Proceedings of the Symposium Robotics in Forestry - Forest Operations in the Age of Technology*, number SR-75, Vaudreuil, Quebec, pp. 36–39.

Lunze, J. (2006). *Regelungstechnik 1 - Systemtheoretische Grundlagen, Analyse und Entwurf einschleifiger Regelungen*, Springer-Verlag, Berlin, Heidelberg.

Morari, M. & Zafiriou, E. (1989). *Robust Process Control*, Prentice-Hall, New Jersey.

Ostoja-Starzewski, M. & Skibniewski, M. (1989). A master-slave manipulator for excavation and construction tasks, *Robotics and Autonomous Systems* **4**: 333–337.

Parker, N. R., Salcudean, S. E. & Lawrence, P. D. (1993). Application of force feedback to heavy duty hydraulic machines, *IEEE International Conference on Robotics and Automation*, Atlanta, pp. 375–381.

Rosenberg, L. B. (1993). Virtual fixtures: Perceptual tools for telerobotic manipulation, *Proceedings of the Virtual Reality Annual International Symposium*, pp. 76–82.

Sachs, S., Teichert, H.-J. & Rentzsch, M. (1994). *Ergonomische Gestaltung mobiler Maschinen*, ecomed-Verlag, Landsberg.

Salcudean, S., Tafazoli, S., Hashtrudi-Zaad, K. & Lawrence, P. D. (1997). Evaluation of impedance and teleoperation control of a hydraulic mini-excavator, *in* A. Casals &

A. T. de Almeida (eds), *Experimental Robotics V, Proceedings of the Fifth International Symposium*, Barcelona, pp. 187–198.

Schwarzmann, D. (2007). *Nonlinear Internal Model Control with Automotive Applications*, Logos Verlag, Berlin.

Tafazoli, S., Salcudean, S. M., Hashtrudi-Zaad, K. & Lawrence, P. D. (2002). Impedance control of a teleoperated excavator, *IEEE Transactions on Control Systems Technology* **10**(3): 355–367.

Uchino, H., Takada, M., Shimizu, T., Shibayama, M. & Furuno, F. (1977). System for controlling a power shovel, *Patent US 4059196*, Hokushin Electric Works.

Wallersteiner, U., Lawrence, P. & Sauder, B. (1993). A human factors evaluation of two different machine control systems for log loaders, *Ergonomics* **26**(8): 927–934.

Yamada, H. & Muto, T. (2003). Development of a hydraulic tele-operated construction robot using virtual reality (new master-slave control method and an evaluation of a visual feedback system), *International Journal of Fluid Power* **4**(2): 35–42.

Yoshinada, H. & Takeda, S. (1990). Master/slave type manipulator, *Patent US 4893981*, Kabushiki Kaisha Komatsu Seisakusho.

Zhu, M. & Salcudean, S. E. (1995). Achieving transparency for teleoperator systems under position and rate control, *Proc. Intl. Conf. Intelligent Robots and Systems*, Pittburgh, PA, pp. 7–12.

Advances in Haptics

Edited by Mehrdad Hosseini Zadeh

ISBN 978-953-307-093-3
Hard cover, 722 pages
Publisher InTech
Published online 01, April, 2010
Published in print edition April, 2010

Haptic interfaces are divided into two main categories: force feedback and tactile. Force feedback interfaces are used to explore and modify remote/virtual objects in three physical dimensions in applications including computer-aided design, computer-assisted surgery, and computer-aided assembly. Tactile interfaces deal with surface properties such as roughness, smoothness, and temperature. Haptic research is intrinsically multi-disciplinary, incorporating computer science/engineering, control, robotics, psychophysics, and human motor control. By extending the scope of research in haptics, advances can be achieved in existing applications such as computer-aided design (CAD), tele-surgery, rehabilitation, scientific visualization, robot-assisted surgery, authentication, and graphical user interfaces (GUI), to name a few. Advances in Haptics presents a number of recent contributions to the field of haptics. Authors from around the world present the results of their research on various issues in the field of haptics.

InTech Europe
University Campus STeP Ri
Slavka Krautzeka 83/A
51000 Rijeka, Croatia
Phone: +385 (51) 770 447
Fax: +385 (51) 686 166
www.intechopen.com

InTech China
Unit 405, Office Block, Hotel Equatorial Shanghai
No.65, Yan An Road (West), Shanghai, 200040, China
中国上海市延安西路65号上海国际贵都大饭店办公楼405单元
Phone: +86-21-62489820
Fax: +86-21-62489821

IntechOpen